

Bridgewater College

**BC Digital Commons**

---

Honors Projects

---

Spring 2023

## **An Analysis of Energy Production and Efficiency in Various Longbow Archery Models**

Hannah McPherson

hmcpherson@eagles.bridgewater.edu

Follow this and additional works at: [https://digitalcommons.bridgewater.edu/honors\\_projects](https://digitalcommons.bridgewater.edu/honors_projects)



Part of the [Engineering Physics Commons](#), and the [Other Physics Commons](#)

---

### **Recommended Citation**

McPherson, Hannah. "An Analysis of Energy Production and Efficiency in Various Longbow Archery Models." *Senior Honors Projects, Bridgewater College, 2022.*

This Honors Project is brought to you for free and open access by BC Digital Commons. It has been accepted for inclusion in Honors Projects by an authorized administrator of BC Digital Commons. For more information, please contact [rlowe@bridgewater.edu](mailto:rlowe@bridgewater.edu).



# AN ANALYSIS OF ENERGY PRODUCTION AND EFFICIENCY IN VARIOUS LONGBOW ARCHERY MODELS

**Hannah McPherson**

Advisor: Dr. Deva O'Neil

Bridgewater College

Fall 2022

## **Abstract**

An analysis of the energy production and efficiency of three lab-tested longbow models is undertaken. The first model, which is constructed to not allow flexing of limbs and which uses a frictionless cart and track in place of an arrow, demonstrated an efficiency of 50% +/- 40%. The second model, which is constructed similarly to the first with the exception of a wooden dowel now being used as an arrow-like object, demonstrated an efficiency of 13% +/- 3%. The last model, a 3D printed longbow with flexible limbs using the wooden dowel as an arrow-like object, demonstrated an efficiency of 40% +/- 10%. A conclusion that may be drawn from this data, as well as from the values of work and kinetic energy contained herein, is that the flexibility of the limbs increases the energy efficiency of the bow. The results from the second and third models in particular, may explain how the flexible limbs of a real longbow facilitate the transfer of stored energy directly into kinetic energy, lowering the total amount of energy lost through other forms, such as vibrational in the strings.

## **I. General Background**

The bow and arrow have long been tools of humanity for hunting, war, and entertainment. With its many uses, the bow has evolved into a more complex tool throughout history, with innovative technologies still being used today to develop a more efficient system in terms of energy production and transfer.

The longbow is the most basic version of the bow. Traditionally made using a single piece of strong but flexible wood, such as yew, this tool stores the majority of its potential energy in the flex of two curved limbs at either end of the centered grip<sup>1</sup>. This flex is produced by the pulling of a string attached to both limbs during the draw cycle. As the longbow is drawn, some amount of energy is produced by the force required to move the string a certain distance. This energy becomes strain that is then stored in both the flexing limbs as well as the string itself, which becomes tauter than when the system is at a relaxed position. The focus of this research, however, is on what happens once the string is released. Upon release, the stored energy is dispersed, with some becoming kinetic energy transferred to the arrow, propelling it forward. While much of the energy stored within the bow is transferred to the arrow in an efficient model, there is some dispersed in the string as vibrations while it snaps back into its resting position. A small amount of energy is also given off as heat from the system. Therefore, it is important to focus on the work produced by the system during the time after the string is released from its taut position up until the arrow loses contact with the string. Through this, it would then be possible to determine how much energy is kinetic, and how much is lost through other means for several types of archery models. Additionally, the efficiency of the model itself may be found in terms of how much of the energy put into the longbow leaves in the form in kinetic energy.

Before continuing the discussion on energy and efficiency, a few terms must be defined. One important characteristic of bows is *brace height*<sup>2</sup>. This measurement refers to the distance between the center point of the bow grip and the main string in resting position<sup>2</sup>. The *draw length* of the bow may be determined from measuring the furthest point on the string at full draw, which is where the arrow should be nocked, to the center of the bow's grip, subtracting the brace height. Both of these features are outlined in *figure 1* below. This relationship can therefore be described as

$$\Delta d - b = l, \tag{1}$$

where  $d$ ,  $b$ , and  $l$  represent displacement, brace height, and draw length, respectively.

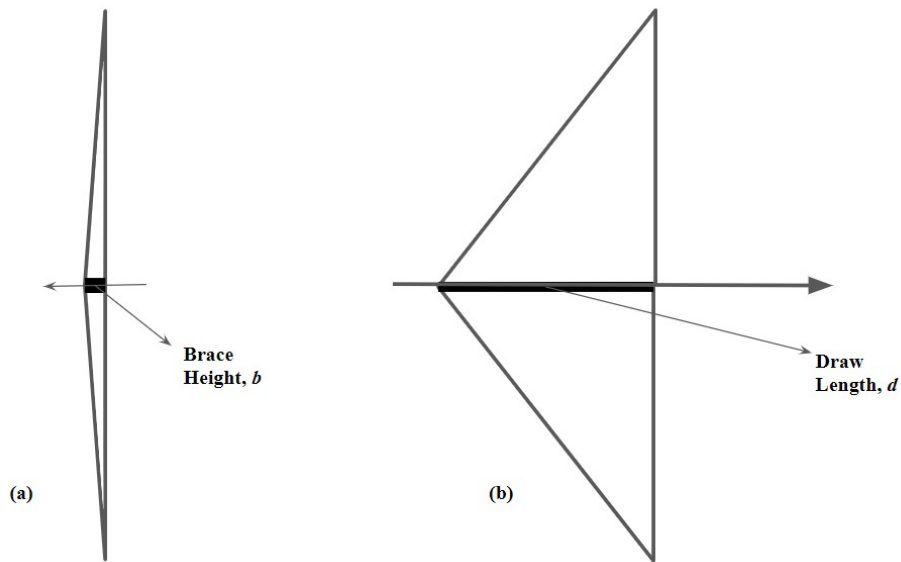


Figure 1. (a) Diagram of longbow model in undrawn position, highlighting brace height; (b) Diagram of longbow model in drawn position, displaying draw length. The distance that the bow was drawn back may be found by subtracting these two values.

In the context of this paper, the brace height was used as the origin point of measurements for horizontal distance measurements, as the arrow was found to lose contact with the string after this point.

Another constant of importance in the following models is string angle. At full draw on all models of a longbow, the location where the arrow is connected to the string will form a decisive angle with either ends of the string both above and beneath it. If the arrow is in the exact middle of the string, as is the norm, this angle will be the same on either side. For the sake of accuracy when firing any bow model, it is important that the string angle is the same each draw cycle, as this allows for a consistent draw length and weight, producing an accurate shot by eliminating variance between cycles. This constant will be discussed more in the following sections on theory due to its importance in the calculations for determining work in the bow/arrow system.

## **II. Theory**

### **Kinetic Energy Calculations**

Herein it is important to note that an analysis of the energy present in the system after to the release of the string is being undertaken. Therefore, the following calculations are relevant in the time between release and the time at which the string reaches the brace height, which is where the arrow disconnects from the string and has been labeled as the origin of our system.

In order to calculate the kinetic energy present in the system at any given time,  $t$ , the standard formula for classical motion is applied,

$$KE = \frac{1}{2}mv^2 .$$

Here, the mass,  $m$ , is the mass of the arrow in kg, and the velocity,  $v$ , is taken in m/s, allowing for a kinetic energy value in Joules. Note that this unit convention will be applied throughout this paper. This value of kinetic energy may be calculated for multiple intervals during the period listed above. In order to find the velocity of the arrow/string system for each interval, it may be assumed that

$$V = \frac{\Delta x}{\Delta t}, \tag{3}$$

where velocity is equal to the ratio of change in distance,  $x$ , over change in time,  $t$ .

### **Work Calculations**

The second value that is intended to be analyzed in this research, work, may be found in the following way for each of the intervals used in the calculations for kinetic energy:

$$W = F\Delta x, \tag{4}$$

where the force,  $F$ , is the net force of the string/arrow system during each interval denoted by position,  $x$ . In order to find this net force, the string angle must be calculated. This may be undertaken by following the diagram listed below. Once the string angle,  $\theta$ , is found in radians, the net force of the interval may be calculated.

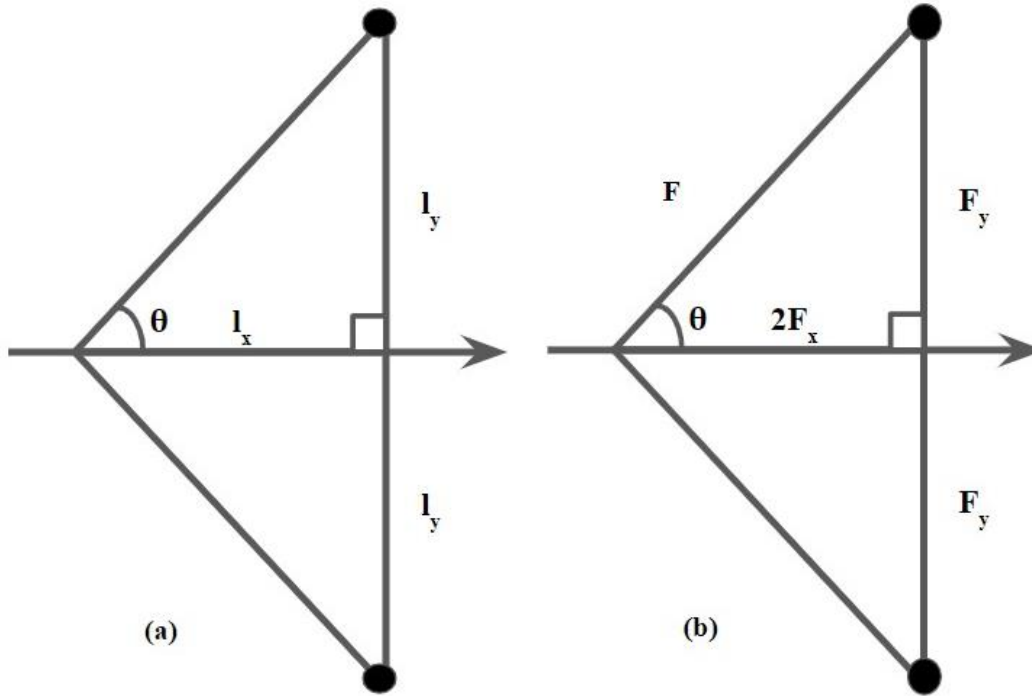


Figure 2. (a) Position Diagram of standard longbow at drawn position; (b) Force Diagram of standard longbow at drawn position. Both diagrams share the same value for  $\theta$ .

Following the diagrams in *figure 2*, the horizontal and vertical values referenced may be known through data collection. In the case of a non-bending bow, the value for  $l_y$  will stay constant for the entirety of the release cycle. The collection of values for  $l_x$  will be discussed below in the experimental section. In order to calculate work, however, we will need to find the net force on the string. This value,  $F_{net}$ , will rely on the value for  $F_x$ , as the vertical force,  $F_y$ , will cancel itself out on either side of the string, being as it is equal in magnitude but opposite in direction. The value of force,  $F$ , which will be found experimentally, must be used alongside the value for  $\theta$  for the given interval in order to solve for  $F_x$ . Therefore, using the *figure 2b* above, it may be assumed that

$$F_{net} = F_{hyp} x = 2F_{hyp} \cos(\theta).$$

In order to complete this calculation, one must first find the value for  $\theta$  in the given interval. This may be done according to the diagram found in *figure 2a* in accordance with

$$\theta = \arccos\left(\frac{l_x}{l_y}\right). \tag{6}$$

Once the string angle is found, *equation 5* may be implemented to find the net force along each interval of the release cycle. Note that the string angle will change with each interval, so these values must be recalculated at each value of  $\Delta t$ .

### **Efficiency**

At the conclusion of calculations for kinetic energy and work, an analysis of the system's efficiency will be undertaken according to the below equation,

$$\eta = \frac{\Delta KE}{W_{net}}. \tag{7}$$

For the value of  $\Delta KE$ , it is crucial that value for the last interval is used for this calculation. This way, the total efficiency of the model may be found. It is important to note, however, that the value for  $W_{net}$  is our total energy input, or the sum of all energy in the system according to *equation 8*,

$$W_{net} = \Delta KE + E, \tag{8}$$

where  $E$  denotes other forms of energy that may be produced during the release cycle, such as vibrational energy in the string or thermal energy dispersed from the system.

### III. Experiment

#### Model One; Non-flexing Limbs with Frictionless Cart

##### *Materials*

- (1) PASCO Wireless Force Acceleration Sensor with Hook Attachment
- (1) Laptop with PASCO Capstone Software and Video Camera
- (1) PASCO Wireless Smartcart
- (1) Frictionless Cart Track
- (1) 1.2m Steel Rod
- (2) 0.303m Steel Rods, 0.012m diameter
- (2) Orthogonal Boss Head Clamps
- (1) C-Clamp
- (1) Large Bench Clamp
- (1) Ruler
- 0.65m Flexible String, 0.003m diameter

For the experimental portion of the project, three different systems were assembled and evaluated. The first, pictured in *figure 3* below, was made up of a longbow-type model that relied only on the flex in the string for energy production. With a typical longbow, the string is anchored at either end by flexible limbs that allow for a greater energy capacity. In this case, however, the system was created by attaching a large metal rod to a table in a vertical position. To this rod, two smaller bars were attached horizontally, 0.62m apart. The string was attached to the model 0.18m along the horizontal rods, measured from the vertical beam. At the bottom, the string was tied into place and wrapped to prevent sliding. On the top rod, however, a PASCO Force Detector was attached at the 0.18m point using a clamp. A hook was then screwed onto the detector, which allowed for the top end of the string to be securely looped on.



*Figure 3. Experimental setup one, longbow model without flexible limbs with frictionless cart and track as arrow-like object (left); Experimental setup two, longbow model without flexible limbs with wooden dowel as arrow-like object (right).*

In place of an arrow, this first experiment was completed with a small frictionless cart on a track instead. This choice was made in order to create a baseline for data collection. Due to the high mass of the cart, the video analysis was capable of producing a greater number of frames to analyze during the needed period, allowing for more data to work with. Additionally, this object, when used in conjunction with the friction-less track, was a model similar to that of a regular archery arrow during the draw and release cycles. As far as the cart and track placement is concerned, the rod and string setup outlined above was situated so that the middle of the string was level with the stopper on the end of the cart when it was resting on the track placed on a tabletop. This step is crucial so that the string angle is the same both above and below the place the cart is touching the string every time.

For data collection, it has already been mentioned that a PASCO Force detector was in use. This data was supplemented by position measurements collected by using CAPSTONE software with video analysis. This allowed for a video to be taken during the experiment, with time values during said video correlating to simultaneous collection of force data from the detector. It is important to note that a scale must be defined in order to execute proper video analysis. In the case of this experiment, a ruler was placed in the same place as the track. Using video analysis tools, it was then possible to determine the distance the cart traveled during each interval, allowing for the appropriate energy and work calculations to take place. These intervals were determined to be the frame rate used to record the video, which was 0.033 seconds. Another matter to note here is that when using the CAPSTONE software in conjunction with the PASCO Force Detector in this experiment, it is necessary to change the collection speed of said detector to a higher rate. For this and the following experiments, this value was set to the max, 1kHz.

## **Model Two; Non-flexing Limbs with Wooden Dowel**

### *Materials*

- (1) PASCO Wireless Force Acceleration Sensor with Hook Attachment
- (1) Laptop with PASCO Capstone Software and Video Camera
- (1) 0.46m Wooden Dowel, 0.09m diameter
- (1) 1. 2m Steel Rod
- (2) 0.303m Steel Rods, 0.012 diameter
- (2) Orthogonal Boss Head Clamps
- (1) C-Clamp
- (1) Large Bench Clamp
- (1) Ruler
- 0.65m Flexible String, 0.003m diameter

For the second longbow model, which can also be seen in *figure 3* above, the assembly was altered to use a wooden dowel as an arrow-like object in place of the cart used previously. This

change allowed for an object of smaller mass to be launched, while still using something of an arrow-like shape. An important note on the dowel, however, is that it was necessary to carve a small notch into one end to simulate a “nock” which is a small piece on the end of an arrow that connects it to the string. In the case of this experiment, this was included in order to fit the dowel to the string during the draw and release cycle, making it much simpler to analyze when the arrow left the string during the video analysis stage. Due to the low mass of an actual arrow, it was decided to use the dowel in order to allow for a video analysis to remain possible. In addition, the overall length of the longbow model was decreased to 0.52m in order to keep the velocity of the dowel low while still allowing for a substantial change in horizontal position from the brace height when pulling back the string. The anchor points of the string for both the top and the bottom of the model were kept 0.18m from the main rod. Furthermore, the data collection method for these trials were kept constant from the first experiment, using a combination of the force detector and video analysis to acquire values for force, time, and distance during the intervals determined by the frame rate. In order to maintain lab safety, the wooden dowel was fired into a sizable box a short distance away in order to prevent accidental damage of lab equipment or observers.

### **Model Three; Flexing Limbs with Wooden Dowel**

#### *Materials*

- (1) PASCO Wireless Force Acceleration Sensor with Hook Attachment
- (1) Laptop with PASCO Capstone Software and Video Camera
- (1) Computer with access to SOLIDWORKS and Qidi Print Software
- (1) QIDI X-MAX Printer
- (1) PLA Printed Longbow
- (1) 0.46m Wooden Dowel, 0.009m diameter
- (1) C-Clamp
- (1) Ruler
- 0.65m Flexible String, 0.003m diameter



*Figure 4: Experimental setup 3, 3D printed longbow model with flexible limbs (left); Flexible longbow limbs, designed using SOILDWORKS and printed using PLA filament (right).*

The third experimental setup, shown above in *figure 4*, involved allowing flex in the limbs of a longbow. In order to achieve this, a small longbow model was created in Solidworks and 3D printed using PLA filament in a Qidi X-Max printer. The object was then evaluated using the same wooden dowel from experiment two as the arrow-like object. The design of the longbow limbs was such that two identical limbs may be printed and inserted into a small grip, which was also made of two interlocking pieces, allowing for a longer model to be created without exceeding the parameters of the printer bed. In addition, the limbs were designed to have a small notch near their ends in order to keep the string from changing position during the draw cycle. Once assembled, the longbow model had the string anchored on the top at the pre-printed notch.

On the bottom limb, however, the Force Detector was attached using a clamp, with the string attached to the detector's hook in line with the pre-printed notch. In order to maintain lab safety, the wooden dowel was again fired into a sizable box a short distance away in order to prevent accidental damage of lab equipment or observers. The data collection for this experiment was kept constant to that of the previous two.

#### IV. Results & Discussion

##### Error Propagation

An in-depth discussion of the results of this research will require additional calculations for error propagation of the resultant values of kinetic energy, work, and efficiency. The first propagation to be completed is the uncertainty in work values. According to *equations 4- 6*, it can be seen that work is related to the value of  $\theta$  for each interval. Therefore, the uncertainty calculations for work must start with an evaluation of the uncertainty in  $\theta$ , which may be found by

$$\Delta\theta = \sqrt{\left(\frac{\delta\theta}{\delta x}\right)^2 \Delta x^2 + \left(\frac{\delta\theta}{\delta y}\right)^2 \Delta y^2} . \tag{9}$$

In order to find the values for the derivatives, one must first take a look at the governing equation for the calculation of  $\theta$ , *equation 6* from above. From this, it can be determined that the derivative of  $\theta$  with respect to the x position of a given point is

$$\frac{\delta\theta}{\delta x} = -\frac{y}{x^2(1+\frac{y^2}{x^2})} . \tag{10}$$

For the second term,  $\theta$  with respect to the y position of the string/arrow system, it can be assumed that there is negligible uncertainty due to this value being measured repeatedly in the lab for the

experiments outlined below. Therefore, after eliminating that term and simplifying algebraically from *equation 9*, we are left with

$$\Delta\theta = \frac{\delta\theta}{\delta x} \Delta x = -\frac{y}{x^2(1+\frac{y^2}{x^2})} \Delta x. \quad (11)$$

Now that the absolute uncertainty of  $\theta$  has been derived, we may begin solving the absolute value of the horizontal force uncertainty,

$$\Delta F_x = \sqrt{\left(\frac{\delta F_x}{\delta\theta}\right)^2 \Delta\theta^2 + \left(\frac{\delta F_x}{\delta F_{hyp}}\right)^2 \Delta F_{hyp}^2} \quad (12)$$

Taking the above derivatives with respect to  $\theta$  and  $F_{hyp}$  from *equation 5* yields

$$\frac{\delta F_x}{\delta\theta} = -2F_{hyp} * \sin\theta, \text{ and} \quad (13)$$

$$\frac{\delta F_x}{\delta F_{hyp}} = 2 * \cos\theta. \quad (14)$$

Using the values calculated for theta and  $F_{hyp}$  from experimental data, *equation 12* may now be solved for a numerical value of absolute uncertainty of horizontal force,  $F_x$ . In order to calculate work, however, the fractional uncertainty of  $F_x$  must be obtained. This may be found through

$$\delta F_x = \frac{\Delta F_x}{F_x}. \quad (15)$$

Also needed for the calculation of uncertainty for work is the fractional uncertainty of the string/arrow x-position,

$$\delta x = \frac{\Delta x}{x}. \quad (16)$$

It is important to note that the value for  $x$  used in the above formula should be the change in distance over the given interval, rather than a single position point. Now that the values for uncertainty in  $F_x$  and  $x$  have both been determined, work uncertainty may be found by

$$\delta w = \sqrt{\delta F_x^2 + \delta x^2}. \quad (17)$$

Using the solution found in *equation 17*, absolute uncertainty of work can be determined according to *equation 18*,

$$\Delta w = \delta w * w. \quad (18)$$

The concluding calculation in this series is to find the absolute uncertainty of the net work done in the system,

$$\Delta w_{net} = \sqrt{\Sigma(\Delta w^2)}. \quad (19)$$

The next value to calculate uncertainty for is velocity. From *equation 3*, it is known that velocity in the context of this research is found through the change in distance over the change in time. Therefore, the uncertainty for these values must be found in order to calculate that of velocity. For the change in time, fractional uncertainty can be found by

$$\delta t = \frac{\sqrt{\Delta t_b^2 + \Delta t_c^2}}{t} = \frac{\sqrt{2}\Delta t}{t}. \quad (20)$$

Note that for the above equation, the absolute uncertainty of all intervals of time are the same, so it may be simplified for the change in time to have a factor of root two when calculating the fractional uncertainty from a ratio of absolute uncertainty and the time interval. This may also be

applied to the calculation of fractional uncertainty in  $x$ , as the values will be the same for each interval as well, giving

$$\delta x = \frac{\sqrt{2}\Delta x}{x}. \quad (21)$$

Now, these values may be combined into

$$\delta v = \sqrt{\delta t^2 + \delta x^2}. \quad (22)$$

From there, the absolute uncertainty of the velocity of a given interval may be determined by

$$\Delta v = v * \delta v. \quad (23)$$

Given that the absolute uncertainty of velocity has now been derived, the uncertainty in kinetic energy must also be considered. Conveniently, the uncertainty for  $KE_{net}$  of the system is calculated very similarly to that of  $W_{net}$ . Following *equation 24* below, it can be seen that the partial derivatives of both variables in the kinetic energy formula (found in *equation 2*) are necessary. These terms are shown in *equations 25 and 26*, allowing a numerical answer for the fractional uncertainty in kinetic energy for each interval. This value can then be used to determine the absolute uncertainty for the kinetic energy.

$$\delta KE = \sqrt{\left(\frac{\delta KE}{\delta m}\right)^2 \Delta m^2 + \left(\frac{\delta KE}{\delta v}\right)^2 \Delta v^2} \quad (24)$$

$$\frac{\delta KE}{\delta m} = \frac{1}{2}v^2 \quad (25)$$

$$\frac{\delta KE}{\delta v} = mv \quad (26)$$

$$\Delta KE = KE * \delta KE \tag{27}$$

Finally, the uncertainty of the net kinetic force during the release cycle may be determined by

$$\Delta KE_{net} = \sqrt{\Sigma(\Delta KE)^2}. \tag{28}$$

The concluding calculation for this section will be deriving the absolute uncertainty of the efficiency of the model. From *equation 7*, it can be seen that said efficiency is a ratio of the change in kinetic energy output in the final interval of the cycle and the total work calculated over all intervals. Since the absolute uncertainty for both of these values has already been calculated, the calculation will start with

$$\delta \eta = \sqrt{\delta KE^2 + \delta w_{net}^2}, \tag{29}$$

where the fractional uncertainties for kinetic energy and net work are given by

$$\delta KE = \frac{\Delta KE}{KE}, \text{ and} \tag{30}$$

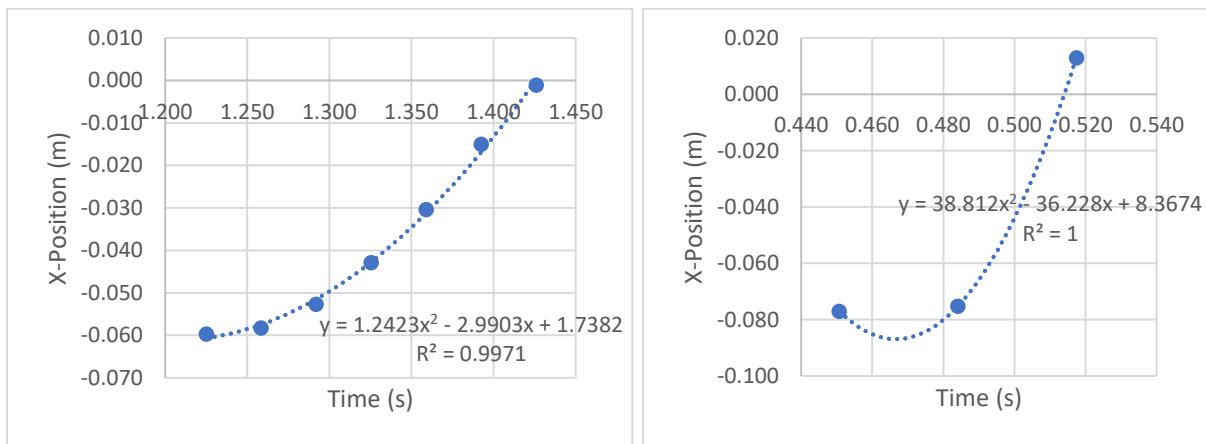
$$\delta w_{net} = \frac{\Delta w_{net}}{w_{net}}. \tag{31}$$

Lastly, the absolute uncertainty of the model's efficiency will be determined by

$$\Delta \eta = \delta \eta * \eta. \tag{32}$$

To begin the analysis of the data collection from the experiments listed above, one may first take a look at the position graphs of the three models. In *figure 5*, these graphs may be observed. For all three models, the relationship between the changes in position and time follow a quadratic fit rather than linear. This demonstrates that the velocity for each time interval is changing, and in

the case of the graphs in *figure 5*, said velocity is increasing. For the first model, the quadratic fit of the graph is generated using seven data points. Since the  $R^2$  value for this graph is remarkably close to one, it can be assumed that this fit is accurate. Therefore, for this model it is possible to determine the x-position of the cart/string system (measured at the point the cart touches the string) for any time during the release cycle. For the second model, however, only three data points were observed due to the low frame rate used for the video analysis. Unfortunately, this makes it difficult to tell if the fit is truly accurate, so additional testing of the model in a way to gain more data points to necessary to draw a reasonable conclusion. In the case of the third model, the quadratic curve is created using five data points, resulting in a decent fit. Like the first model, this means that the x-position of the arrow/string system (measured at the point that the arrow touches the string) can be determined for any time during the release cycle. Further analysis of this trend can be taken by referencing the raw data and calculations from the experiments in *Appendices A-C*. Note that the values of kinetic energy and work also increase with time, which is in line with increasing values of velocity.



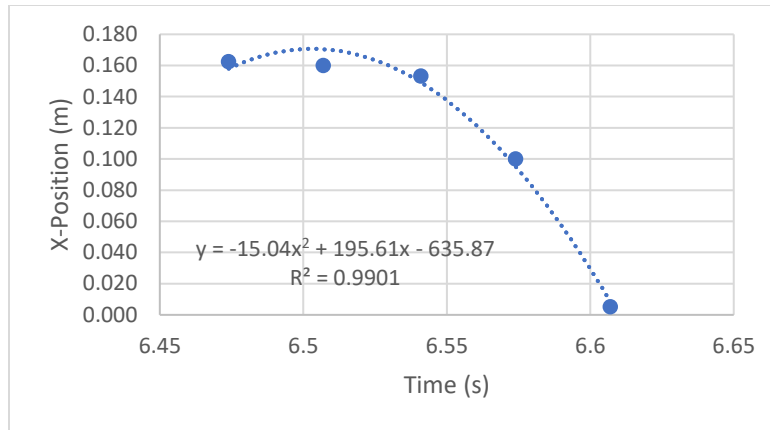


Figure 5: Position versus time graph of non-flexing limbs model using the cart and track in place of an arrow (top left); Position versus time graph of non-flexing limbs model using wooden dowel (top right); Position versus time graph of flexing limb model using wooden dowel (bottom).

Furthermore, a look into the calculated values for  $W_{\text{net}}$ ,  $KE_{\text{net}}$ , and final velocity should also be taken. For the first, non-flexing model, the  $W_{\text{net}}$  was found to be  $0.05 \pm 0.04\text{J}$ . In comparison,  $KE_{\text{net}}$  for this model was  $0.087 \pm 0.001\text{J}$ . Therefore, the kinetic energy measured in the string/arrow system was greater than the total work done in the system, or the energy that was put into it. While this result seems implausible, the high value of uncertainty for  $W_{\text{net}}$  means that it is possible that the total work of the system could be a much greater value than what was calculated. The calculated final velocity of this first model was found to be  $0.4 \pm 0.6\text{ m/s}$ , which was much lower than in subsequent models. Additionally, there is again a high uncertainty, being more than the value itself. This is due to uncertainty in the x-position of the string/cart system, as the low frame rate of the video made analysis difficult due to blurring of the cart.

For the second model, the values for  $W_{\text{net}}$  and  $KE_{\text{net}}$  were found to be  $0.6 \pm 0.2\text{J}$  and  $0.0781 \pm 0.0008\text{J}$ , respectively. In this case, the work put into the system was much greater than the total kinetic energy calculated to have exited. This is a plausible result, as the string was observed to have high vibration after the dowel was disconnected at the end of the release cycle, demonstrating

that there should have been a large amount of energy lost. The final velocity of the string/dowel system for this model was calculated to be  $2.6 \pm 0.6$  m/s, which is a significantly higher value than in the previous model. Additionally, the value for uncertainty remains the same, but it now is a lower percentage of the velocity itself.

In the third model, similar calculations were completed. The values of  $W_{\text{net}}$  and  $KE_{\text{net}}$  were found to be  $0.23 \pm 0.06$ J and  $0.122 \pm 0.004$ J, respectively, while the final velocity of the system was calculated to be  $2.9 \pm 0.7$  m/s. In this case, it can be seen that while the total work in the system is greater than the total kinetic energy, there is a smaller difference between the two than in the previous model. In the non-flexing wooden dowel system, the total kinetic energy of the system made up only 13% of the total work, omitting uncertainties. In contrast, the flexing model used in experiment three yielded total kinetic energy that made up 53% of the total work in the system, omitting uncertainties. These values hint at a trend in efficiencies of the various systems, which will be discussed in the following paragraphs.

A further analysis of these models involves comparing the calculated values of efficiency for all three experiments. In the first model, which was assembled to eliminate any flex in limbs and used a friction-less cart and track in place of an arrow, there was found to be great efficiency. This efficiency, a ratio of change in kinetic energy and overall energy input as in *equation 7*, was calculated to be  $50\% \pm 40\%$ . Due to the high value of uncertainty for this model, it is difficult to draw any reasonable conclusions from the data. From the error bars, the value of efficiency for this mode could be either exceedingly small, resulting in an inefficient system in which very little of the energy present is converted into kinetic energy, or it could lead to a very efficient system in which the majority of energy present is converted into kinetic energy. Therefore, additional testing

of this model, minimizing error gained in the uncertainty of the x-position, is required in order to draw a valid conclusion.

In the second model, which was again assembled to eliminate any flex in limbs but replaced the cart and track with a wooden dowel, the same efficiency calculations were undertaken. Out of the three trials for this model, the highest value for efficiency was 13% +/- 3%. During the experiment, this model had a noticeable increase in string vibration compared to the previous. Additionally, it was observed to be much louder during the release cycle, leading to an inefficient system as energy was dispersed in vibrations in place of kinetic energy propelling the dowel forward.

In the third model, which was assembled in a way to allow for the flexing of limbs, most closely simulating that of a typical longbow, the efficiency with the dowel had a bit of variance between trials. The highest value was found to be 40% +/- 10%. Herein, it can be determined that the system is efficient in comparison to the non-flexing dowel model, however it is inefficient in comparison to the non-flexing model utilizing the cart and track.

An analysis of the second and third models, which utilized an arrow-like object, can be compared to real world models. For example, the low value of efficiency in the second model, which did not use flexible limbs, compared to the higher value found in the model that did use flexible limbs could suggest some reasoning behind the typical design component of having flexible bow limbs. Not only do the limbs seem to store energy, but they also help to facilitate the transfer of the potential energy directly into kinetic, mitigating the amount lost through other forms and creating a more efficient model than that of a non-flexing longbow.

Overall, the values for uncertainty found from the data have the potential to be reduced. For example, the uncertainty for x-position was assumed to be 0.015m, as the low frame rate of the video made accurate analysis difficult. This in turn affected the uncertainty of all subsequent uncertainty calculations. In order to solve this issue, a video camera with a higher frame rate could be used in future trials in order to refine the results from the three models. Additionally, another solution could involve using a position motion sensor in real-time in conjunction with the force detector in order to eliminate the need for video analysis altogether. The assumed values of uncertainty for x-position, time, and force were 0.015m, 0.001s, and 0.00001N, respectively for all models.

## **V. Future Directions**

Further work on this material could include repeated trials of the three experiments listed above with a camera capable of a greater frame rate in order to allow for more intervals, especially in regard to the second and third experiments. In these cases, more accurate representations could be modeled from an increase in data.

Furthermore, another avenue of research may stem from pursuing more efficient longbow models, encouraging a dive into how and why the longbows of today are made, and if they can be improved upon. For example, research into how the longbows used in the modern Olympics differ from those used in past centuries may be of interest in terms of the total efficiency of the system.

Subsequent research may also be conducted in regard to the draw cycle of a longbow. For instance, the experimental setups from above may be reevaluated for work and energy values throughout the draw cycle instead of the release cycle. This data may then be compared to that of the release cycle, to observe if there are any noticeable changes in the potential energy stored in the bow system and that which is converted to kinetic upon release of the string.

## **VI. Works Cited**

1. Ledsoe, Colin. "Designing a Better Archery Bow." *International Conference on Engineering and Product Design*. (2018).
2. McDougal, Darron. "What is Brace Height and Why is it Important." *Bowhunting.com*. (2019).  
<https://www.bowhunting.com/bowhunt-101/2019/08/27/what-is-brace-height-and-why-is-it-important/>

## Appendix A

*The following is raw data as well as calculation results collected in three trials using the first model outlined in the experimental section: non-flexing limbs with cart/track arrow substitution.*

### Trial 1

X-Position (m)	Force (N)	Time (s)
-0.059641353785992	-3.814727711395870	1.225
-0.058248631656170	-3.793848229813610	1.259
-0.052664741873741	-3.772968748233630	1.292
-0.042897373437881	-3.747270924750580	1.326
-0.030339367687702	-3.732815899041370	1.359
-0.014993242919445	-3.760119836492110	1.393

L <sub>x</sub> (m)	L <sub>y</sub> (m)	θ (radians)	F <sub>x</sub> (N)
0.060	0.308	1.380	1.450430572
0.058	0.308	1.384	1.409983858
0.053	0.308	1.401	1.271817133
0.043	0.308	1.432	1.033839585
0.030	0.308	1.473	0.731855811
0.015	0.308	1.522	0.365647478
0.001	0.308	1.567	0.025295576

ΔX (m)	ΔT (s)	V (m/s)	KE (J)	KE <sub>net</sub> (J)
0.0014	0.034	0.04156	0.00023	0.00023
0.0056	0.034	0.16661	0.00378	0.00401
0.0098	0.034	0.29144	0.01155	0.01556
0.0126	0.034	0.37471	0.01910	0.03466
0.0153	0.034	0.45790	0.02852	0.06317
0.0140	0.034	0.41642	0.02358	0.08676

W (J)	W <sub>net</sub> (J)
0.002020	0.002020
0.007873	0.009893
0.012422	0.022316
0.012983	0.035299
0.011231	0.046530
0.005103	0.051633

## Trial 2

X-Position (m)	Force (N)	Time (s)
-0.052779801189899	-4.60654189746500	0.505
-0.052779801189899	-4.59851132762655	0.538
-0.051416337490082	-4.57923796001426	0.571
-0.044599033892155	-4.55146250498915	0.605
-0.033691331744194	-4.49720033694362	0.638

$L_x$ (m)	$L_y$ (m)	$\theta$ (radians)	$F_x$ (N)
0.0528	0.308	1.401	1.556
0.0528	0.308	1.401	1.553
0.0514	0.308	1.405	1.508
0.0446	0.308	1.427	1.305
0.0337	0.308	1.462	0.978
0.0173	0.308	1.515	0.503

$\Delta X$ (m)	$\Delta T$ (s)	V (m/s)	KE (J)	KE <sub>net</sub> (J)
0.000000000000000	0.033	0	0	0
0.001363463699817	0.033	0.040904	0.000227554	0.000227554
0.006817303597927	0.033	0.204519	0.005688837	0.005916392
0.010907702147961	0.033	0.327231	0.014563468	0.02047986
0.016361534595489	0.033	0.490847	0.032767727	0.053247587

W (J)	W <sub>net</sub> (J)
0.000000	0.000000
0.002118	0.002118
0.010281	0.012399
0.014229	0.026628
0.016002	0.042630

### Trial 3

X-Position (m)	Force (N)	Time (s)
-0.195256963372231	-4.569601276208120	0.706
-0.182923495769501	-4.543903452725070	0.739
-0.158256635069847	-4.508568945435890	0.772
-0.113034084439278	-4.492507805758980	0.805
-0.051366925239563	-4.479658894074550	0.839

$L_x$ (m)	$L_y$ (m)	$\theta$ (radians)	$F_x$ (N)
0.195	0.308	1.006	4.893
0.183	0.308	1.035	4.641
0.158	0.308	1.096	4.121
0.113	0.308	1.219	3.096
0.051	0.308	1.406	1.474

$\Delta X$ (m)	$\Delta T$ (s)	$V$ (m/s)	KE (J)	KE <sub>net</sub> (J)
0.012	0.0333	0.37	0.018704386	0.018704386
0.025	0.0333	0.74	0.074817092	0.093521478
0.045	0.0333	1.36	0.251468257	0.344989735
0.062	0.0333	1.85	0.46760694	0.812596675

$W$ (J)	$W_{net}$ (J)
0.060352006	0.060352006
0.114468718	0.174820724
0.18636292	0.361183644
0.190894728	0.552078372

### Additional Notes:

- All three trials shared the constant value of 0.308m for  $L_y$ , referenced in figure 2.
- The mass of the cart was found to be 0.27201kg.

## Appendix B

*The following is raw data as well as calculation results collected in three trials using the second model outlined in the experimental section: non-flexing limbs with wooden dowel.*

### Trial 1

X-Position (m)	Force (N)	Time (s)
-0.076973587274551	-3.984975791968780	0.451
-0.075204581022263	-3.601114553690750	0.484

$L_x$ (m)	$L_y$ (m)	$\theta$ (radians)	$F_x$ (N)
0.076973587	0.2575	0.206576144	7.800501785
0.075204581	0.2575	0.290155542	6.901171511

$\Delta X$ (m)	$\Delta T$ (s)	$V$ (m/s)	KE (J)	$KE_{net}$ (J)
0.001769006252288	0.033	0.053007	3.13986E-05	3.13986E-05
0.088223546743393	0.033	2.643545	0.078094573	0.078125972

$W$ (J)	$W_{net}$ (J)
0.013799136	0.013799
0.608845827	0.622645

### Trial 2

X-Position (m)	Force (N)	Time (s)
-0.035688817501068	-3.58184118607847	0.611
-0.033949673175812	-3.55774947656311	0.644

$L_x$ (m)	$L_y$ (m)	$\theta$ (radians)	$F_x$ (N)
0.035688818	0.2575	1.34637193	1.594243346
0.033949673	0.2575	3.6241833	6.302877955

$\Delta X$ (m)	$\Delta T$ (s)	$V$ (m/s)	KE (J)	$KE_{net}$ (J)
0.005286842584610	0.033	0.159553	0.000284483	0.000284483
0.068721830844879	0.033	2.07397	0.048067611	0.048352094

W (J)	W <sub>net</sub> (J)
0.002772619	0.002773
-0.164606797	0.167379

### Trial 3

X-Position (m)	Force (N)	Time (s)
-0.049555957317352	-3.719966987299840	0.688
-0.044269114732742	-3.639661288915320	0.722

L <sub>x</sub> (m)	L <sub>y</sub> (m)	θ (radians)	F <sub>x</sub> (N)
0.049555957	0.2575	-1.903326962	-2.42866
0.044269115	0.2575	-0.503556694	6 37575

ΔX (m)	ΔT (s)	V (m/s)	KE (J)	KE <sub>net</sub> (J)
0.005286842584610	0.033	0.159553	0.000284483	0.000284483
0.068721830844879	0.033	2.07397	0.048067611	0.048352094

W (J)	W <sub>net</sub> (J)
-0.01284	-0.01284
0.438153	0.425314

### Additional Notes:

- All three trials shared the constant value of 0.2575 for L<sub>y</sub>, referenced in figure 2.
- The mass of the wooden dowel was found to be 0.02235kg.

## Appendix C

*The following is raw data as well as calculation results collected in three trials using the third model outlined in the experimental section: flexing limbs with wooden dowel.*

### Trial 1

X-Position (m)	Force (N)	Time (s)
0.211815804243088	-2.43025747124438	5.164
0.207477182149887	-2.37316026504450	5.197
0.205307930707932	-1.60150266391607	5.231

$L_x$ (m)	$L_y$ (m)	$\theta$ (radians)	$F_x$ (N)
0.211815804243088	0.273828923702240	0.912403209	2.97389
0.207477182149887	0.278180837631226	0.929965742	2.83764
0.205307930707932	0.278180837631226	0.934995186	1.90202

$\Delta X$ (m)	$\Delta T$ (s)	$V$ (m/s)	KE (J)	KE <sub>net</sub> (J)
0.004338622093201	0.033	0.131473397	0.000193163	0.000193163
0.002169251441955	0.034	0.063801513	4.54893E-05	0.000238652
0.095450460910798	0.033	2.892438209	0.093492272	0.093730924

W (J)	W <sub>net</sub> (J)
0.012903	0.012903
0.006156	0.019058
0.181548	0.200606

### Trial 2

X-Position (m)	Force (N)	Time (s)
0.162410497665405	-2.43346969917976	6.474
0.160099744796753	-2.38689239411673	6.507
0.153167784214020	-2.07530628438478	6.541
0.100021958351135	-1.58222929630379	6.574

$L_x$ (m)	$L_y$ (m)	$\theta$ (radians)	$F_x$ (N)
0.162410497665405	0.278599083423614	1.043004824	2.451120158
0.160099744796753	0.278599083423614	1.049217616	2.378536141
0.153167784214020	0.278599083423614	1.068123195	1.999339442
0.100021958351135	0.276288390159607	1.223453542	1.077183238

$\Delta X$ (m)	$\Delta T$ (s)	V (m/s)	KE (J)	KE <sub>net</sub> (J)
0.002310752868652	0.033	0.070022814	5.47932E-05	5.47932E-05
0.006931960582733	0.034	0.203881194	0.000464517	0.00051931
0.053145825862885	0.033	1.610479572	0.028983977	0.029503287
0.094737887382507	0.033	2.870845072	0.092101572	0.121604859

W (J)	W <sub>net</sub> (J)
0.005663933	0.005663933
0.016487919	0.022151852
0.10627249	0.128424341
0.102050064	0.230474406

### Trial 3

X-Position (m)	Force (N)	Time (s)
0.229949384927750	-2.56517104453038	8.683
0.225305408239365	-2.56171044530381	8.716
0.209051579236984	-2.30979892366759	8.749

L <sub>x</sub> (m)	L <sub>y</sub> (m)	$\theta$ (radians)	F <sub>x</sub> (N)
0.229949384927750	0.282197117805481	0.887063605	3.240791
0.225305408239365	0.282197117805481	0.897033424	3.196661
0.209051579236984	0.284519106149673	0.93712421	2.735301

$\Delta X$ (m)	$\Delta T$ (s)	V (m/s)	KE (J)	KE <sub>net</sub> (J)
0.004643976688385	0.033	0.140726566	0.000221309	0.000221
0.016253829002381	0.033	0.492540273	0.002711009	0.002932
0.083590984344482	0.034	2.458558363	0.067547391	0.07048

W (J)	W <sub>net</sub> (J)
0.01505	0.01505016
0.051958	0.067008145
0.228646	0.295654616

### Additional Notes:

-The mass of the wooden dowel was found to be 0.0223kg